Modal Analysis of Multi-Connected Waveguides

Lorenzo Carbonini

Abstract—**A general analysis for the modal characterization of multi-connected uniform, hollow, conducting waveguides is presented. It is relevant to waveguides with an "outer" conductor for which analytical Green's functions are known and "inner" conductors described by integral equations. The TEM modes space is analyzed, and singularities of the integral equations are studied for determining the higher order modes. The cases of parallel wires into rectangular waveguides and above a ground plane are worked in detail; experimental results about a complex multi-wire line are reported. Mixed coaxial and circular offset coaxial waveguides are also analyzed. Spurious solutions arise due to the structure of the integral equations for multi-connected waveguides; criteria to discard such modes are presented.**

I. Introduction

A GENERAL analysis for the modal characterization of multi-connected uniform, hollow, conducting waveguides is presented; it is relevant to waveguides with an outer conductor for which the Green's functions are known (possibly including the free space case), and inner conductors represented by currents which are solutions of integral equations. The approach shares some aspect with that of [1]; however, in this work the attention is on the potentials rather than on the electric field. In fact, the integral equations arise from boundary conditions of the potentials, which assume a unitary aspect in this formalism.

The TM and TE modes are studied; the resonance conditions are met if the linear operator (frequency dependent) associated to the integral equation is singular, i.e., it has no inverse. This occurs only at the cutoff frequencies, and from a functional viewpoint the kernel of the operator is the resonant current.

The transverse electromagnetic (TEM) modes are studied as a limit of the TM case; a definition of the characteristic impedance in a particular case is stated and a basis of the TEM vector space with a physical meaning is determined for wire lines.

The integral formulation for TE and TM modes is the same as that of [2], [3] if the free space Green's function is used. Various coaxial waveguides are analyzed by use of a moment method (MM) approach analogous to that of [3], and a good agreement with the literature is found; a comparison with the techniques of [2] is presented. Some results about the modal features of offset circular waveguides are shown.

Manuscript received January 2, 1991; revised November 1, 1991.

The author is with Alenia Sistemi Difesa, Gruppo Sistemi Elettromagnetici, Strada Privata dell'Aeroporta, 10072 Caselle Torinese, Italy.

IEEE Log Number 9106045.

The theory is further applied to the case of parallel wires into rectangular waveguides and above a ground plane. The results about the characteristic impedance agree with those found in the literature (e.g., [4]), and have been validated also by MM techniques. Experimental results about a complex multiwire transmission line above a ground plane exhibit a good agreement with the theoretical analysis.

II. Boundary Conditions for the Potentials

The vector potential A and the scalar potential ϕ are related to the electric and magnetic field as follows:

$$\begin{aligned} H &= \nabla \times A \\ E &= -\nabla\phi - j\omega\mu \cdot A, \end{aligned} \tag{1}$$

where ω is the angular frequency, μ is the medium permeability.

With the conventions of Fig. 1, the boundary conditions in uniform conducting waveguides are (for a comparison, see [5]):

$$n \cdot H = 0 \Rightarrow \frac{\partial}{\partial c} A_z - \frac{\partial}{\partial z} A_c = 0 \tag{2a}$$

$$n \times E = 0 \Rightarrow \nabla_\tau \phi + j\omega\mu A_\tau = 0 \tag{2b}$$

where A_τ is the tangential potential vector and ∇_τ is the gradient along the conductor surface; c is the transverse tangent unit vector, $A_c = c \cdot A$ and $\partial/\partial c = c \cdot \nabla$. It should be noted that (2a) is a direct consequence of (2b) if $\omega \neq 0$; in the following (2b) will be used as boundary condition for the potentials.

Every field is assumed to depend on z as $\exp(-j\alpha z)$, where $\alpha^2 = k^2 - k_t^2$; $k = \omega\sqrt{\epsilon\mu}$ is the wavenumber, k_t the cut-off wavenumber for the mode under study, ϵ the medium permittivity. The z dependence will be neglected in the two-dimensional problem and k is replaced by k_t in every expression.

The potential A generated by a current density J for canonical geometries is expressed by an analytical dyadic Green's function G:

$$A(\rho) = -\iint_S d\rho'\, G(k, \rho, \rho') \cdot J(\rho') \tag{3}$$

$$n(\rho) \times A(\rho) = 0 \quad \text{if } \rho \text{ is on the conductor surface}$$

where S is the waveguide section and $\rho = (x, y)$ the coordinate vector.

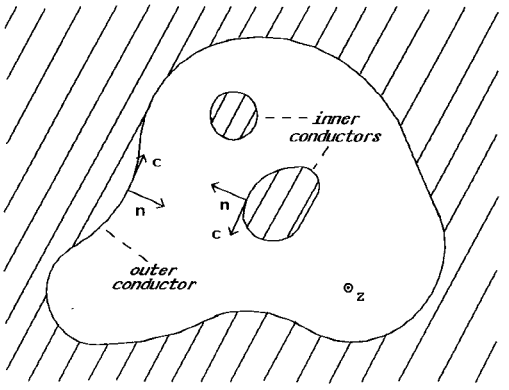

Fig. 1. Geometry of the general multi-connected waveguide.

The analogous expression for the potential ϕ is

$$\phi(\rho) = -1/\epsilon \cdot \int\int_S d\rho'\, g(k, \rho, \rho') \cdot \sigma(\rho') \tag{4}$$

$$\phi(\rho) = 0 \quad \text{if } \rho \text{ is on the conductor surface}$$

where g is the scalar Green's function, $\sigma(\rho) = -\nabla \cdot \boldsymbol{J}/j\omega$ is the charge density.

Every Green's function satisfies the boundary conditions specified by (3) and (4) only on the surface of one conductor, which will be termed the "outer" conductor (a radiation condition in free space).

In the solution procedure a canonical outer conductor is to be singled out together with the corresponding Green's functions; the remaining "inner" ones are represented by tangential electric current distributions. Finally, the solution currents are obtained by enforcing the boundary conditions (2b) at the inner conductors surface.

III. TM Modes

It may be verified from direct substitution into Maxwell equations that both the electric current on the inner conductors and the potential vector are longitudinal; moreover, $\sigma(\rho) = 0$ and $\phi = 0$. Equation (2b) becomes

$$A_z(\rho) = 0 \tag{5}$$

The boundary conditions of A_z on the outer conductor are the same as those of the potential ϕ, and the Green's function g defined in (4) may be used. If L inner conductors are present, (5) may be expressed as

$$\sum_{r'=1}^{L} -\int_0^{s_{r'}} ds'\, g(k_t, \rho_r(s), \rho_{r'}(s')) \cdot J_{r'}(s') = 0 \qquad (r = 1, \cdots, L) \tag{6}$$

where J_r is the (longitudinal) current density on the rth conductor parametrized by $\rho_r(s)$ $(0 \le s \le s_r)$, s is the arc length.

If the linear operator involved is denoted by L^M, (6) may be written as $L^M(J) = 0$. From the theory of linear operators it is well-known that a necessary condition for the existence of nontrivial solutions J of (6) is that L^M has no inverse. The operator is singular only if a resonance occurs; in this case, the currents which are annihilated by L^M are just the resonant ones which generate the higher order mode.

If I_r is the total current of the rth conductor, (6) implies:

$$\underline{Z}_k \cdot \underline{I} = 0. \tag{7}$$

The impedance matrix $\underline{Z}_k$ is defined by

$$(\underline{Z}_k)_{rr'} = -Z_0 \cdot \int_0^{s_r} ds \int_0^{s_{r'}} ds'\, g(k_t, \rho_r(s), \rho_{r'}(s')) \cdot b_r(s) \cdot b_{r'}(s') \tag{8}$$

where $Z_0 = \sqrt{\mu/\epsilon}$ is the medium characteristic impedance and $J_r(s) = I_r \cdot b_r(s)$.

In the case of wire lines the current is constant along the wire surfaces; $b_r(s) = 1/s_r$, and the current densities functionally depend only on L parameters. Equation (6) is equivalent to (7), and may be written as $\det(\underline{Z}_k) = 0$.

The Green's functions for bounded regions usually depend on k as k^2; as a consequence, both k_t and $-k_t$ are solutions of (6) corresponding to the same resonant current.

Unbounded regions exhibit peculiar properties; e.g., in free space the Green's function g is the Hankel function $H_0^{(2)}(k|\rho - \rho'|)$. The wavenumber k_t is complex; this fact is ultimately due to the power loss which occurs by radiation in the far field. In this case, the symmetry is $k_t \to -k_t^*$, where * denotes the complex conjugate, due to the property of the Hankel function $H_0^{(2)}(z^* e^{-j\pi}) = -[H_0^{(2)}(z)]^*$ (e.g., [5]); the resonant currents are complex conjugate. These properties have been extensively studied in singularity expansion methods (SEM, e.g., [7]).

IV. TE Modes

The current in this case is transverse, i.e., $\boldsymbol{J} \cdot \boldsymbol{z} = 0$, and is parallel to the vector $\boldsymbol{c}$ (Fig. 1); the full (2b) has to be taken into account to find the higher order TE modes.

By use of (3), (4) and the properties of the arc-length parametrization choice, (2b) assumes the following form:

$$\sum_{r'=1}^{L} \left\{ \frac{\partial}{\partial s} \int_0^{s_{r'}} ds'\, g(k_t, \rho_r(s), \rho_{r'}(s')) \cdot \sigma_{r'}(s') + j\omega\mu \cdot \int_0^{s_{r'}} ds'\, \boldsymbol{c}_r(s) \cdot \boldsymbol{G}(k_t, \rho_r(s), \rho_{r'}(s')) \cdot \boldsymbol{c}_{r'}(s')\, J_{r'}(s') \right\} = 0. \tag{9}$$

The solutions of (9) exhibit the same symmetry properties of TM modes, both for bounded and unbounded regions.

In the case of wire lines, the assumption of constant current J eliminates the first term in (9); moreover, the second term is negligible for arbitrarily small conductors. Hence a very low perturbation of the TE modes may be

expected; the validity of this claim has been verified in a particular case [8].

V. TEM Modes

The TEM modes correspond to the limiting case of TM modes as $k_t \to 0$. The only difference is that, from (2b), the potential ϕ on the conductor surface is locally constant (i.e., it varies from a conductor to another only).

In this case the relevant integral equation is

$$\sum_{r'=1}^{L} -Z_0 \cdot \int_0^{s_{r'}} ds'\, g(k_t, \rho_r(s), \rho_{r'}(s')) \cdot J_{r'}(s') = V_r \qquad (r = 1, \cdots, L) \tag{10}$$

where V_r is the potential of the rth conductor; (10) is an integral equation for the current densities of the inner conductors only.

The relationship between the total currents $\underline{I} = \{I_r\}$ and the potentials $\underline{V} = \{V_r\}$ is, in matrix notation:

$$\underline{Z} \cdot \underline{I} = \underline{V} \tag{11}$$

where $\underline{Z}$ is expressed by (8) as $k_t \to 0$.

To define a characteristic impedance Z_c for a multiconnected waveguide, it will be assumed that the inner conductors are all connected at the termination (i.e., $V_r = V_0$, $r = 1, \cdots, L$). The unbalanced characteristic impedance Z_c is the impedance through which the inner conductors are connected at the termination to the outer one without power reflections; it may be obtained by equating the power flowing across every section of the line to the dissipated power at the termination. The following relation holds:

$$Z_c = \underline{I}^t \cdot \underline{Z} \cdot \underline{I} / I_T^2 \tag{12}$$

where I_T is the total current flowing in the terminal load, which is the sum of the currents I_r.

If we regard Z_c as a function of $\underline{I}$, the current $\underline{I}$ solution of (11), when $V_r = V_0$ ($r = 1, \cdots, L$), is a stationary point of the unbalanced impedance Z_c. This result may be verified by differentiating (12) and using (11); moreover, under the assumption that $\underline{Z}$ has positive eigenvalues only, by doubly differentiating (12) it can be shown that the current $\underline{I}$ is a (local) minimum of Z_c.

Finally, it should be noted that the set of TEM potentials generated through (10) depends on L parameters, according to the choice of boundary potentials V_r: hence it is a vector space of finite dimension L.

The following of this section is devoted to the case of wire lines.

It is possible to choose a power basis of the TEM vector space in which the following quadratic functional is diagonal:

$$E(\phi, \psi) = \iint_S d\rho\, \nabla_t \phi(\rho) \cdot \nabla_t \psi(\rho) / (2 \cdot Z_0). \tag{13}$$

The problem is easily solvable by linear algebra techniques because it is equivalent to making diagonal the matrix $(\underline{Z})_{rr'}$, which is proportional to $E(\phi_r, \phi_{r'})$; the potentials ϕ_r are generated assuming $I_r = 1$ on the rth wire and $I_r = 0$ elsewhere. Such a basis has a physical meaning, since the power of a general potential may be expressed as the weighted sum of the powers pertaining to the elements of the vector system.

VI. Analysis of Coaxial Waveguides by the Moment Method

The numerical approach to solve the relevant integral equations by the MM is similar to that of [3]; a Galerkin's procedure is used, with triangle functions as basis and test. The relevant linear system is symmetric. In [3] the double integrals were approximated by a function evaluation on 4×4 points; in this paper a 6×6 points approximation is tried, and a comparison between the Galerkin's procedures and the point-matching solution of [2] is made.

The Muller's method is used to find the zeros of the determinant of the relevant impedance matrix, according to [2].

In Table I a comparison is shown between the method here used and that of [2] for a circular waveguide in the TM and TE cases; the Galerkin's procedures are less accurate, both in the 4×4 and in the 6×6 version, so a greater number of subsections is needed to increase the accuracy. Moreover the impedance matrix computation in the Galerkin's procedure requires, if all the symmetries are taken into account, $\theta(s^2 \cdot N \cdot (N+1)/8)$ evaluations of the Hankel function, while a point-matching solution with asymmetric matrix ([2]) requires $\theta(s \cdot N^2)$ (s is the number of function values computed for evaluating each one-dimensional integral, N is the order of the matrix); if $s > 8$ the point-matching procedure is faster as N increases.

A sufficient accuracy is achieved if the length Δ of each linear subsection of the boundary is subjected to the restriction:

$$k \cdot \Delta \leq 0.50 \tag{14}$$

with possible higher limits for the TM case.

The results about a mixed coaxial waveguide (Fig. 2) in the TE and in the TM case (Table II and III) exhibit a good agreement with those of [2].

Finally, the case of an offset circular coaxial waveguide (Fig. 3) is analyzed; the numerical results are shown in Table IV. A part of the modes are labeled by "S"; these are spurious modes, which represent inner resonances of the inner conductor. These solutions may be discarded by computing the resonant induced current; the currents corresponding to the non-excited conductors are very small, about six orders of magnitude lower than the resonant current. Moreover it has been verified numerically that the spurious frequencies depend only on the geometrical modeling of the 'inner' conductor; hence an efficient numerical code should find the resonant frequencies of the inner conductors as a first step to accurately exclude the spurious solutions when dealing with the complete problem.

TABLE I
CIRCULAR WAVEGUIDE—TE AND TM MODES VALUES OF $k \cdot a$, $N = 40$

Mode	Exact	Ref. [3]	Diff. %	6 × 6 Pts.	Diff. %	Ref. [2]	Diff. %
TE							
1	1.8412	1.8487	0.41	—	—	1.8462	0.27
2	3.0542	3.0676	0.44	—	—	3.0645	0.34
TM							
1	2.4048	2.4147	0.41	2.4130	0.34	2.4111	0.26
2	3.8317	3.8475	0.41	3.8447	0.34	3.8416	0.26

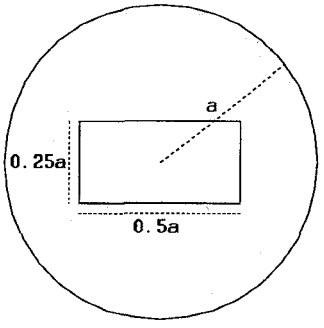

Fig. 2. Mixed coaxial waveguide ([2]).

TABLE II
MIXED COAXIAL WAVEGUIDE—TE MODES VALUES OF $k \cdot a$

Mode	Computed	Ref. [2]	Diff. %
1	1.7453	1.7407	0.26
2	3.0416	3.0441	0.08
3	4.2185	4.2199	0.03
4	4.6311	4.6451	0.30
5	5.2066	—	—

TABLE III
MIXED COAXIAL WAVEGUIDE—TM MODES VALUES OF $k \cdot a$

Mode	Computed	Ref. [2]	Diff. %
1	3.9019	3.8919	0.26
2	4.1717	4.1666	0.12
3	4.4564	4.4450	0.26
4	5.2660	5.2645	0.28
5	6.4277	—	—

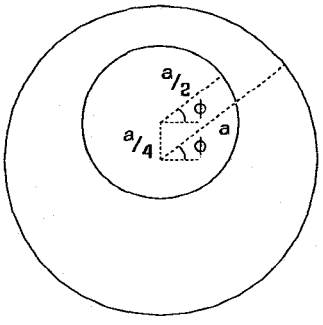

Fig. 3. Offset circular coaxial waveguide.

TABLE IV
OFFSET CIRCULAR COAXIAL WAVEGUIDE—TE AND TM MODES VALUES OF $k \cdot a$

TE	Computed	TM	Computed
1	1.4452	1	4.5517
2	2.6991	*S*1	4.8412
*S*1	3.7063	2	5.3171
3	3.9387	3	6.0397
4	4.7761	4	6.7270
5	5.0963	5	7.3836
6	5.6834	*S*2	7.7130
—	—	6	8.0129

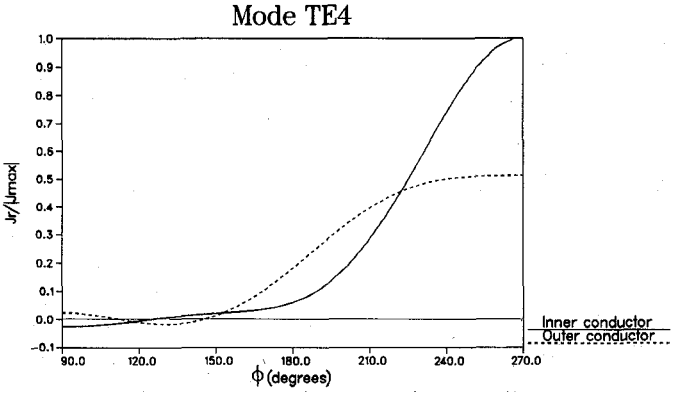

Fig. 4. Current of the TE4 mode of the circular coaxial offset waveguide (Fig. 3).

In comparison with the case of the coaxial circular waveguide, new features in the modal characterization of the offset one appear; in particular, in the case of cylindrical symmetry the inner and outer conductor currents exhibit an equal number of zeros, maxima, and minima.

In the offset waveguide a part of the modes correspond to the symmetric case (TE1, 2, 3, 5, TM2, 4, 6), while the remaining ones exhibit currents which are intrinisically different. The case of the TE4 mode is shown in Fig. 4. It is an open question whether these modes arise by splitting of some degenerate mode or result from the shift toward lower frequencies of very high order symmetric modes.

VII. WIRE LINES INTO RECTANGULAR WAVEGUIDES

The geometry is shown in Fig. 5; the outer conductor is now a rectangular waveguide and the Green's function g is

$$g(k, \boldsymbol{\rho}, \boldsymbol{\rho}') = \frac{4}{a \cdot b} \cdot \sum_{m,n=1}^{\infty} \frac{\sin(k_m x) \cdot \sin(k_m x') \cdot \sin(k_n y) \cdot \sin(k_n y')}{k^2 - k_m^2 - k_n^2} \tag{15}$$

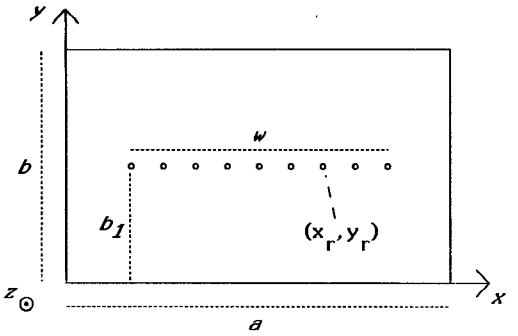

Fig. 5. Geometry of multi-wire lines into a rectangular waveguide.

TABLE V
SINGLE WIRE INTO A RECTANGULAR WAVEGUIDE—PERTURBED TM MODES
VALUES OF $k \cdot b$, $a = 2 \cdot b$, $x_r = b$, $b_1 = b/2$

Mode	Imp. Matrix	MM Solution	Diff. %
$2 \cdot \Delta_r = 0.01 \cdot a$			
1	3.9875	3.9940	0.16
2	6.0773	6.0850	0.13
3	8.6819	—	—
4	9.7804	—	—
5	10.7630	—	—
$2 \cdot \Delta_r = 0.001 \cdot a$			
1	3.8108	3.8203	0.25
2	5.8907	5.8990	0.14
3	8.5936	—	—
4	9.6852	—	—
5	10.6632	—	—

where a and b are the rectangular waveguide dimensions, $k_m = m\pi/a$ and $k_n = n\pi/b$. If wires of square section of sides $2 \cdot \Delta_r$ are located at (x_r, y_r), the TM impedance matrix according to (8) is

$$(\underline{Z}_k)_{rr'} = -\frac{4 \cdot Z_0}{a \cdot b} \cdot \sum_{m,n=1}^{\infty} \frac{\sin(k_m x_r) \sin(k_m x_{r'}) \sin(k_n y_r) \sin(k_n y_{r'})}{k^2 - k_m^2 - k_n^2} \cdot \alpha_{mn}^{r} \cdot \alpha_{mn}^{r'} \tag{16}$$

where the coefficients α_{mn}^{r}, which characterize the wire dimension, are

$$\alpha_{mn}^{r} = \frac{1}{2}\left\{\cos(k_m \Delta_r) \cdot \frac{\sin(k_n \Delta_r)}{k_n \Delta_r} + \frac{\sin(k_m \Delta_r)}{k_m \Delta_r} \cos(k_n \Delta_r)\right\}. \tag{17}$$

The computational efficiency in the evaluation of (16) may be improved by reducing the double sum to a single one by techniques explained in [9]; the analytical results are shown in [8].

The results about the characteristic impedance have been compared with those of [4]; if $d = 1.169 \cdot (2\Delta)$, where d is the equivalent circular wire diameter, the results agree to within 0.01% if $d/a < 0.02$ for a single wire symmetrically sited in a square waveguide. The agreement is within 0.1% for two wires when $d/w < 0.1$ and $w/a < 0.9$.

The cut-off wavenumbers of TM modes are reported in Table V for a symmetric single wire line, in which the $TM_{2m+1,2n+1}$ modes only are perturbed, and compared with the results obtained by MM. Table VI collects the results for a symmetric two-wire line, in which the $TM_{m,2n+1}$ modes only are perturbed. The numerical resolution by MM proved to be difficult due to the sharpness of the zeros of the function to be evaluated.

TABLE VI
TWO WIRES INTO A RECTANGULAR WAVEGUIDE—PERTURBED TM MODES
VALUES OF $k \cdot b$, $a = 2 \cdot b$, $w = b$, $b_1 = b/2$

Mode	Imp. Matrix	MM Solution	Diff. %
$2 \cdot \Delta_r = 0.01 \cdot a$			
1	3.9905	3.9962	0.14
2	5.3426	5.3475	0.09
3	6.0794	—	—
4	9.7821	—	—
5	10.9025	—	—
$2 \cdot \Delta_r = 0.001 \cdot a$			
1	3.8138	—	—
2	4.9673	—	—
3	5.8918	—	—
4	8.5949	—	—
5	9.6868	—	—

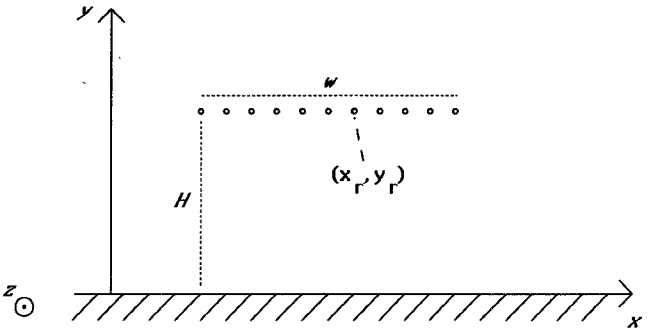

Fig. 6. Geometry of multi-wire lines above a ground plane.

VIII. WIRE LINES ABOVE A GROUND PLANE

The geometry is shown in Fig. 6; the outer conductor is now the ground plane, and the relevant Green's function g is

$$g(k, \boldsymbol{\rho}, \boldsymbol{\rho}') = \frac{1}{2\pi^2} \int_{-\infty}^{+\infty} d\zeta \int_{-\infty}^{+\infty} d\xi \frac{\sin(\xi y) \cdot \sin(\xi y')}{k^2 - \zeta^2 - \xi^2} \cdot \exp(-j\zeta(x - x')) \tag{18}$$

The TM modes impedance matrix according to (8) is

$$(\underline{Z}_k)_{rr'} = -\frac{Z_0}{2\pi^2} \int_{-\infty}^{+\infty} d\zeta \int_{-\infty}^{+\infty} d\xi \frac{\sin(\xi y_r) \cdot \sin(\xi y_{r'})}{k^2 - \zeta^2 - \xi^2} \cdot \exp(-j\zeta(x_r - x_{r'})) \cdot \alpha_{\zeta\xi}^{r} \cdot \alpha_{\zeta\xi}^{r'} \tag{19}$$

where the coefficients $\alpha^{r}_{\xi\xi}$, in analogy with (17), are

$$\alpha^{r}_{\xi\xi} = \frac{1}{2}\left\{\cos(\zeta\Delta_r)\cdot\frac{\sin(\xi\Delta_r)}{\xi\Delta_r} + \frac{\sin(\zeta\Delta_r)}{\zeta\Delta_r}\cdot\cos(\xi\Delta_r)\right\}. \quad (20)$$

The computational evaluation of (19) may be improved by reducing the double integral to a single one by complex plane integration techniques; results for the static impedance matrix are shown in the Appendix.

The results about the characteristic impedance have been compared with those of [4]; if $d = 1.163 \cdot (2 \cdot \Delta)$, where d is the equivalent circular wire diameter, the results agree to within 0.01% when $H/d > 3$, both for a single wire and for a couple of wires.

The complex cutoff wavenumbers for TM modes are found by using an impedance matrix different from that of (19) to avoid the computation of complex integrals; the Green's function for the half-space was used:

$$g(k, \boldsymbol{\rho}, \boldsymbol{\rho}') = -j/4 \cdot [H_0^{(2)}(k|\boldsymbol{\rho} - \boldsymbol{\rho}'|) - H_0^{(2)}(k|\boldsymbol{\rho} - \boldsymbol{\rho}^{*\prime}|)] \quad (21)$$

where $H_0^{(2)}$ is the Hankel function of 2nd kind of order 0, and $\boldsymbol{\rho}^{*\prime} = (x', -y')$. A point-matching approximation is used, in the sense that for each element of the impedance matrix the potential is evaluated at the wire center. The procedure to find the zeros of det $(\underline{Z}_k)$ is similar to that of the previous section, except for the need to calculate complex rather than real wavenumbers.

The results for a single-wire line above a ground plane are reported in Table VII. As could be expected from SEM analyses, the zeros are grouped into layers in the complex k plane; the imaginary part of k increases as the wire diameter decreases.

The computed values for a two-wire line are reported in Table VIII where the symmetry of the induced currents is identified. In the frequency domain SEM framework [7] the current induced by an arbitrary excitation of the wire line is described as an expansion in the resonant currents, whose coefficients are proportional to $1/(k - k_t)$. It is remarkable that the cutoff frequency of the lower order antisymmetric modes has a large imaginary part; hence the contribution of these resonances to the current expansion at real excitation frequencies should be less important than that of the symmetric modes, and a balanced TEM transmission line is expected to provide a wider frequency band than a balanced one.

Finally, a complex multiwire transmission line above a ground plane was designed by use of these techniques; the shape of the central section is shown in Fig. 7, and the wire diameters were chosen in order to yield a 200 Ω balanced characteristic impedance. It is a balanced transmission line, and the outer wire array works as a shield of the inner TM fields; the VSWR in Fig. 8 is less than 2 over a wide frequency band, a good result considering the complexity of the structure and the termination problems. Moreover, field measurements of the TEM mode inside the line have shown an agreement better than 1.5 dB with the theoretical results.

TABLE VII
SINGLE WIRE ABOVE A GROUND PLANE—TM MODES VALUES OF $k \cdot H$

Mode	$2 \cdot \Delta_r = 0.01 \cdot H$	$2 \cdot \Delta_r = 0.001 \cdot H$	$2 \cdot \Delta_r = 0.0001 \cdot H$
1	2.8857 + 1.1006j	2.8008 + 1.2941j	2.7532 + 1.4738j
2	6.0830 + 1.1939j	5.9890 + 1.4131j	5.9423 + 1.5699j
3	9.2569 + 1.2439j	9.1516 + 1.4808j	9.1029 + 1.6469j
4	12.4233 + 1.2769j	12.3067 + 1.5274j	12.2556 + 1.7009j
5	15.5857 + 1.3011j	15.4583 + 1.5628j	15.4048 + 1.7423j
6	18.7459 + 1.3200j	18.6080 + 1.5911j	18.5521 + 1.7757j

TABLE VIII
TWO WIRES ABOVE A GROUND PLANE—TM MODES VALUES OF $k \cdot H$, $w = \frac{2}{3} \cdot H$, $2 \cdot \Delta_r = 0.01 \cdot H$

Mode	Computed	Parity
1	0.5568 + 1.8545j	O
2	2.9521 + 0.6344j	E
3	3.7270 + 1.7467j	O
4	5.7892 + 0.7964j	E
5	6.9491 + 1.3116j	O
6	9.7284 + 1.0825j	O
7	12.2038 + 0.9664j	E
8	12.8284 + 1.2458j	O
9	15.0404 + 1.0334j	E
10	16.0874 + 1.0891j	O
11	18.1773 + 1.3646j	E

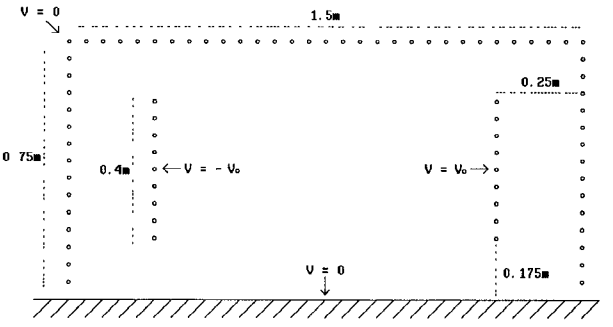

Fig. 7. Central section of the designed multiwire transmission line.

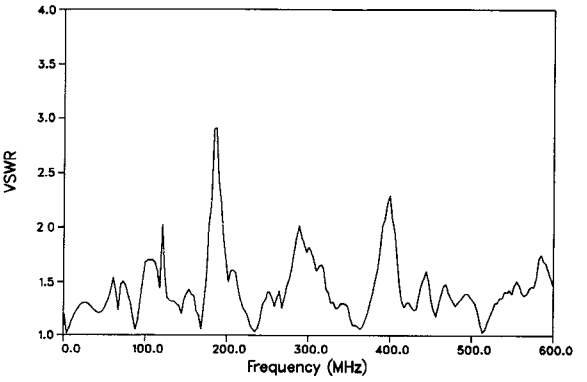

Fig. 8. Measured VSWR of the transmission line.

IX. CONCLUSION

The theoretical setting for a complete modal characterization of multi-connected, uniform, hollow, conducting waveguides has been established. The numerical analysis

is performed only on the inner conductors; this approach leads to a considerable reduction of the degrees of freedom of the problem, provided that the Green's functions of the outer conductor are known. Moreover, it has been verified that in the case of wire lines in rectangular waveguides a standard MM solution to the problem is very difficult; the numerical efficiency of the algorithm is greatly improved by the present approach, according to [1].

The numerical procedures for determining the higher order modes of multi-connected waveguides with a surface integral formulation always exhibit spurious solutions at the inner conductor resonant frequencies; two criteria to discard without any doubt such modes have been proposed.

The analysis of waveguides whose spatial domain is unbounded shares many aspects with SEM techniques (e.g., [7]); it has been verified (mainly in time domain problems) that an expansion of the currents in the base of complex resonant currents gives correct results (see also [10]). A complete study in the SEM framework of waveguides whose spatial domain is unbounded would lead to an exact modal characterization of these geometries, in analogy with the classical analysis of closed waveguides by means of orthogonal functions; however the required functional analysis techniques are very complex.

Finally, it is thought that a careful characterization of useful basis for the vector space of TEM modes in wire lines may lead to simple criteria in establishing optimization algorithms for some parameters of the problem (e.g., TEM mode field uniformity, or impedance properties); further analyses should be carried on in this direction.

Appendix

It is possible to reduce the double integral in (19) to a single one; the convergence of the integral is exponential for off-diagonal matrix elements, quadratic for diagonal ones. The residues theorem and Jordan's lemma are used; only the relevant results are shown. The static impedance matrix is considered.

If $|y_r - y_{r'}| > |x_r - x_{r'}|$ it is useful to perform the ξ integration to achieve a fast converging ζ integral; the result is

$$(\underline{Z})_{rr'} = -Z_0/(2\pi) \cdot \int_0^{+\infty} d\zeta \cos(\zeta|x_r - x_{r'}|) \cdot [\exp(-\zeta|y_r + y_{r'}|) - \exp(-\zeta|y_r - y_{r'}|)] \cdot \frac{\gamma_\zeta^r \cdot \gamma_\zeta^{r'}}{\zeta} \quad \text{(A1)}$$

which is valid if $|y_r - y_{r'}| > \Delta_r + \Delta_{r'}$; γ_ζ^r may be obtained by replacement of ξ with j_ζ in $\alpha_{\zeta\xi}^r$ ((21)).

In the dual case, the result is

$$(\underline{Z})_{rr'} = Z_0/\pi \cdot \int_0^{+\infty} d\xi \sin(\xi y_r) \cdot \sin(\xi y_{r'}) \cdot \exp(-\xi|x_r - x_{r'}|) \cdot \frac{\gamma_\xi^r \cdot \gamma_\xi^{r'}}{\xi} \quad \text{(A2)}$$

which is valid if $|x_r - x_{r'}| > \Delta_r + \Delta_{r'}$; γ_ξ^r may be obtained by replacement of ζ with $j\xi$ in $\alpha_{\xi\xi}^r$.

Finally, if the matrix element is diagonal, the procedure is slightly different. The final result is

$$(\underline{Z})_{rr} = Z_0/(4\pi) \cdot \int_0^{+\infty} d\xi \sin^2(\xi y_r) \cdot \beta^r/\xi \quad \text{(A3)}$$

where

$$\beta^r = \sin(\xi\Delta_r)/(\xi\Delta_r) \cdot [\cosh(\xi\Delta_r) \cdot \sin(\xi\Delta_r)/(\xi\Delta_r) + 2 \cdot \cos(\xi\Delta_r) \cdot \sinh(\xi\Delta_r)/(\xi\Delta_r)] \cdot \exp(-\xi\Delta_r) + \cos^2(\xi\Delta_r) \cdot [1 - \exp(-\xi\Delta_r) \cdot \sinh(\xi\Delta_r)/(\xi\Delta_r)]/(\xi\Delta_r). \quad \text{(A4)}$$

References

[1] G. Conciauro, M. Bressan, and C. Zuffada, "Waveguide modes via an integral equation leading to a linear matrix eigenvalue problem," *IEEE Trans. Microwave Theory Tech.*, vol. MTT-32, pp. 1495–1504, Nov. 1984.

[2] M. Swaminathan *et al.*, "Computation of cutoff wavenumbers of TE and TM modes in waveguides of arbitrary cross sections using a surface integral formulation," *IEEE Trans. Microwave Theory Tech.*, vol. 38, pp. 154–159, Feb. 1990.

[3] B. Spielman and R. F. Harrington, "Waveguides of arbitrary cross section by solution of a nonlinear integral eigenvalue equation," *IEEE Trans. Microwave Theory Tech.*, vol. MTT-20, pp. 578–585, Sept. 1972.

[4] L. T. Lo and S. W. Lee, Eds., *Antenna Handbook*. New York: Van Nostrand, 1988, pp. 28.13–28.18.

[5] L. F. Jelsma *et al.*, "Boundary conditions for the four vector potential," *IEEE Trans. Microwave Theory Tech.*, vol. MTT-18, pp. 648–649, Sept. 1970.

[6] M. Abramowitz and I. Stegun, *Handbook of Mathematical Functions*. New York: Dover, 1965, p. 361.

[7] L. Marin, "Natural-mode representation of transient scattered fields," *IEEE Trans. Antennas Propagat.*, vol. AP-21, pp. 809–818, Nov. 1973.

[8] L. Carbonini, "Theoretical and experimental analysis of a multi-wire rectangularly shielded transmission line for EMC measurements," in *Proc. IEEE Int. Symp. on EMC*, Cherry Hill, NJ, August 1991.

[9] R. E. Collin, *Field Theory of Guided Waves*. New York: McGraw-Hill, pp. 580–589, 1961.

[10] F. M. Tesche, "On the analysis of scattering and antenna problems using the singularity expansion technique," *IEEE Trans. Antennas Propag.*, vol. AP-21, pp. 53–62, Jan. 1973.

Lorenzo Carbonini was born in Vercelli, Italy, on June 17, 1965. He received the physics degree cum laude from Università degli Studi, Turin, Italy, in 1989.

He has been with Alenia Sistemi Difesa, Caselle Torinese (TO), Italy, since 1989. His fields of interest include multiconnected waveguides, transmission line devices for EMC measurements, radar cross section analysis, electromagnetic properties of materials, spectral techniques in scattering problems, analytical and numerical techniques in electromagnetic problems.